13.42; H, 1.69; N, 7.83. Found: C, 13.99; H, 1.16; N, 7.51.

$ThBr_4(DME)_2$ (6). A 3.00-g (3.57-mmol) amount of $ThBr_4(THF)_4$ was placed in a 125-mL Erlenmeyer flask and 20 mL of toluene added. To this slurry was then added 5 mL of DME, and the resulting suspension stirred at room temperature for 24 h. The white solid was filtered off onto a frit and pumped dry. Yield: 2.10 g (80%). IR (Nujol, cm^{-1}): 1456 (s), 1288 (w), 1256 (m), 1246 (w), 1188 (m), 1152 (w), 1116 (m), 1084 (s), 1010 (vs), 852 (vs), 844 (s), 830 (m). ^1H NMR (300 MHz, C_6D_6): δ 3.83 (s, 6 H, O*Me*), 3.41 (s, 4 H, CH_2O). Anal. Calcd for $C_8H_{20}Br_4O_4Th$: C, 13.13; H, 2.75. Found: C, 13.61; H, 1.60.

Crystallographic Studies: $ThBr_4(THF)_4$. Crystal data, collection, and processing parameters are given in Table I. Since crystal decomposition occurred at room temperature, presumably due to loss of solvent trapped in the lattice, the data were collected at −40 °C. A crystal measuring 0.20 × 0.15 × 0.20 mm was coated in Nujol and mounted on a glass fiber under an argon purge. The fiber was then placed on the goniometer head of an Enraf-Nonius CAD-4 diffractometer in a −40 °C nitrogen cold stream. Graphite-monochromated Mo Kα radiation was used. Unit cell parameters were determined from the least-squares refinement of $((\sin \theta)/\lambda)^2$ values for 24 accurately-centered reflections. Two reflections were chosen as intensity standards and measured every 150 reflections. Data were collected by ω scans.

Equivalent reflections were merged, and systematically absent reflections were rejected. The structure was solved by routine Patterson and Fourier methods. After inclusion of anisotropic thermal parameters for all non-hydrogen atoms and geometrical generation of hydrogen atoms which were constrained to "ride" upon the appropriate carbon atoms, final refinement using 1091 unique observed $[F > 4\sigma(F)]$ reflections converged at $R = 0.037$ and $R_w = 0.042$ {where $w = 1/[\sigma^2(F)^2 + 0.0005F^2]$}. All calculations were performed using the SHELXTL PLUS suite of computer programs (Siemens Analytical X-ray Instruments Inc., 1990). A correction for absorption was applied.[41]

Acknowledgment. We wish to thank Dr. A. P. Sattelberger, Dr. W. G. Van Der Sluys, and Dr. C. J. Burns for helpful discussions and Dr. R. R. Ryan for the generous use of X-ray diffraction facilities. We acknowledge the Office of Basic Energy Sciences, Division of Chemical Sciences, U.S. Department of Energy, under Contract No. W-7405-eng-36 with the University of California and the Yucca Mountain Site Characterization Project Office as part of the Civilian Radioactive Waste Management Program managed by the U.S. Department of Energy, Nevada Operations Office, for financial support.

Supplementary Material Available: For $ThBr_4(THF)_4$, a table of anisotropic thermal parameters (Table S1) (2 pages); a table of crystallographic structure factors (Table S2) (12 pages). Ordering information is given on any current masthead page.

(41) Walker, N.; Stuart, D. *Acta Crystallogr.* **1983**, *A39*, 158. Uguzzli, F. *Comput. Chem.* **1987**, *11*, 109. Katayama, C. *Acta Crystallogr.* **1986**, *A42*, 19.

Contribution from the Department of Chemistry, University of Alberta, Edmonton, Alberta, Canada T6G 2G2

Reactions of Perfluoromethyl-Substituted Cyclopolyphosphines with Zerovalent Group 10 Metal Complexes. Crystal and Molecular Structure of a Complex with a Coordinated Diphosphene, $[Pd(\eta^2\text{-}CF_3P{=}PCF_3)(PPh_3)_2]$

Ian G. Phillips, Richard G. Ball, and Ronald G. Cavell*

Received January 23, 1991

Reactions of trifluoromethyl-substituted cyclopolyphosphines $(CF_3P)_4$ and $(CF_3P)_5$ with zerovalent Pt, Pd, and Ni complexes gave a variety of products under different conditions. The most definitive reactions were those in which $(CF_3P)_4$ reacted with the zerovalent metal complexes under refluxing conditions in benzene to give η^2-CF_3PPCF_3 complexes of the formula $L_2M(CF_3PPCF_3)$. The crystal and molecular structure of $(Ph_3P)_2Pd(\eta^2\text{-}CF_3PPCF_3)$ (monoclinic $P2_1/n$, $Z = 4$, $a = 11.200$ (2) Å, $b = 19.441$ (3) Å, $c = 17.502$ (3) Å, $\beta = 101.71$ (1)°, $R_1 = 0.048$, $R_2 = 0.062$) showed clearly the η^2 adduct in the *E* configuration. The P=P bond length of 2.121 Å is consistent with a coordinated diphosphene as formulated. The CF_3PPCF_3 group can be transferred to different metals (e.g. Pt) by simple metathetical exchange. The various coordinated and ring-opened intermediates formed via initial 1,3-coordination of the cyclic polyphosphines both $(CF_3P)_4$ and $(CF_3P)_5$ and subsequent ring opening were identified by NMR spectroscopy, and some aspects of the mechanism of formation of the intermediates and the final η^2 adduct are discussed.

Introduction

Many examples of transition-metal-induced reductive ring-opening reactions of *cyclo*-$[ER]_n$ (E = P, As) to give homoatomic polyorganophosphorus or -arsenic catenates are known.[1a–d] These polyphosphine–transition metal metallacyclic complexes may also be accessed from reaction of lithiated phosphines with organometallic alkyls or chlorides (eq 1)[1e] (M = Zr, Hf; x = 0, 1, 2)

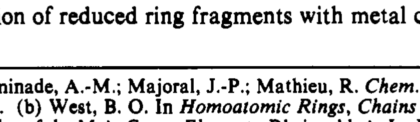

(1)

1

or by reaction of reduced ring fragments with metal chlorides,[1f] such as is shown in eq 2. These reactions are not necessarily

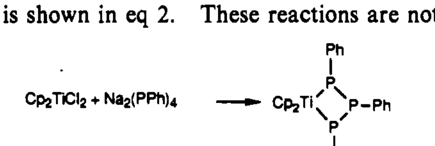

(2)

1c (M=Ti)

stoichiometric. Complexes of η^2-(side-bonded)-diphosphenes (e.g., $L_2Pt(\eta^2\text{-}PhPPPh)$; L = PPh_3 (**2**), dppe (**3**)) are also prepared via a similar route[2] (eq 3). The reactions of $(EC_6F_5)_4$ (E = P, As)

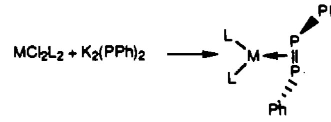

(3)

2,3

with $[Pt(PPh_3)_3]$ (1:1 Pt/"$(C_6F_5P)_2$") in refluxing benzene have been shown to give η^2-diphosphene (or diarsene) compounds $[Pt(\eta^2\text{-}C_6F_5E{=}EC_6F_5)(PPh_3)_2]$[3] (E = P (**4**), As (**5**)). An X-ray

(1) (a) Caminade, A.-M.; Majoral, J.-P.; Mathieu, R. *Chem. Revs.* **1991**, *91*, 575. (b) West, B. O. In *Homoatomic Rings, Chains and Macromolecules of the Main Group Elements*; Rheingold, A. L., Ed.; Elsevier: Amsterdam, 1977; Chapter 18. (c) Rheingold, A. L.; Fountain, M. E. *Organometallics* **1984**, *3*, 1417. (d) Mercando, P.; DiMaio, A.-J.; Rheingold, A. L. *Angew. Chem., Int. Ed. Engl.* **1987**, *26*, 244 and references therein. (e) Hey, E.; Bott, S. G.; Atwood, J. L. *Chem. Ber.* **1988**, *121*, 561. (f) Köpf, H.; Voigtländer, R. *Chem. Ber.* **1981**, *114*, 2731.

(2) Chatt, J.; Hitchcock, P. B.; Pidcock, A.; Warrens, C. P.; Dixon, K. R. *J. Chem. Soc., Chem. Commun.* **1982**, 932; *J. Chem. Soc., Dalton Trans.* **1984**, 2237 and references therein.

0020-1669/92/1331-1633$03.00/0

crystallographic determination has been given for **4**.[3]

Recently Jones et al.[4] reported the preparation of a unique and unusual Ni(II) species (**6**) shown by X-ray crystallography to contain both an η^2-diphosphene and a nickel–phosphorus five-membered ring (eq 4). Formation of the $[Ni(PBu^t)_4]$ ring has

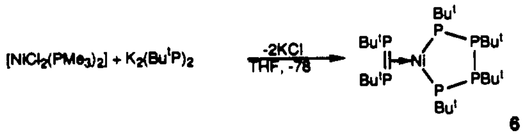

(4)

6

been taken as evidence of a coupling reaction between two diphosphene moieties at the nickel center in a manner analogous to metallacyclopentane formation for alkenes[4] (eq 5). We propose an alternative mechanism which may be more likely.

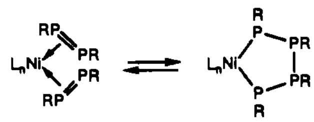

(5)

The coordination chemistry of $(CF_3P)_4$ has not been extensively studied. Burg obtained a polymeric nickel carbonyl complex of the tetramer which proved difficult to characterize.[5] Cowley et al. prepared an iron carbonyl complex $[Fe(CO)_3]_2{\cdot}(CF_3P)_4$ (**7**),[6] which on the basis of infrared spectroscopy and limited NMR parameters was considered to be structurally analogous to $[Fe(CO)_3]_2(\mu\text{-}[CH_3As]_4)$ (**8**).[7] There are no reports of the coordination chemistry of $(CF_3P)_5$ in the literature.

In this investigation we present evidence concerning the probable mechanism of formation of η^2-diorganodiphosphene transition metal complexes in the reaction of $(CF_3P)_{4,5}$ with tertiary phosphine supported Ni(0), Pd(0), and Pt(0). Many unstable intermediate species were identified by ^{31}P and ^{19}F NMR spectroscopy. We have obtained the crystal and molecular structure of the palladium diphosphene complex $[Pd(\eta^2\text{-}CF_3P{=}PCF_3)(PPh_3)_2]$ (**9**), which is a representative member of the series of ultimate products of these reactions, namely bis(trifluoromethyl)diphosphene complexes.

Experimental Section

All reactions were performed in sealed glass tubes, and a combination of standard vacuum-line and Schlenk techniques[8] (argon) was used throughout for the manipulation of volatile compounds and air-sensitive solids. $(CF_3P)_{4,5}$ was prepared[9] by the mercury reduction of CF_3PI_2, which was itself obtained by a standard route.[10] Samples of crystalline $(CF_3P)_4$, pure by ^{19}F NMR spectroscopy, were obtained by repeated distillation of the solids left following decantation of the liquid from mixtures of $(CF_3P)_{4,5}$ in sealed glass tubes. $[Pt(\eta^2\text{-}C_2H_4)(PPh_3)_2]$[11] and $[ML_n]$ (M = Pt, n = 3, L = PEt_3;[12] M = Pt, n = 4, L = PEt_3,[12] PMe_2Ph,[13] PPh_3;[14] M = Pd, n = 4, L = PPh_3;[14] M = Ni, Pd, n = 2, L = $Ph_2PCH_2CH_2PPh_2$[15]) were prepared by published procedures. Benzene and toluene were distilled from drying agents as required.

^{19}F and ^{31}P NMR spectra of solutions were recorded using a Bruker WP400 instrument at the appropriate frequencies, and shifts are referenced to $CFCl_3$ and 85% H_3PO_4, respectively.

General Procedure for Reaction of $(CF_3P)_4$ (or $(CF_3P)_{4,5}$) with Zerovalent Tertiary Phosphine–Ni, –Pd, and –Pt Complexes. The transition metal substrate $[ML_n]$ (approximately 0.1 mmol) was placed in a 5-mm NMR tube. The tube was then evacuated, and toluene or benzene was distilled into the tube. The solvent was melted to allow the solid to dissolve, and then the solution was refrozen. $(CF_3P)_4$ (approximately 0.2 mmol as "$(CF_3P)_2$") was then distilled onto the frozen solution, and the tube was sealed in vacuum. The sample was allowed to slowly warm to room temperature unaided, and then the tube was shaken vigorously to ensure dissolution of the cyclopolyphosphine(s). In all cases (except in the case of $[Ni(dppe)_2]$) the solution became vividly red during this treatment. Evolution of ethylene from the reaction of $[Pt(\eta^2\text{-}C_2H_4)(PPh_3)_2]$ with the cyclopolyphosphines was observed at this stage. The extent and nature of reaction in samples prepared in this way was monitored by means of ^1H, ^{19}F, and ^{31}P NMR spectroscopy, and in many cases intermediate species were observed which were characterized by NMR spectroscopy. Reaction of $[Ni(dppe)_2]$ with *cyclo*-$(CF_3P)_{4,5}$ did not occur without aid of reflux, and formation of intermediates was limited. Platinum or $[Pd(dppe)_2]$ complexes reacted slowly at room temperatures and traversed the range of intermediates noted.

Refluxing solutions of the platinum complexes prepared as described above for ca. 10 min led to a product mixture composed largely of η^2-diphosphene complexes. In the case of $Pd(dppe)_2$ plus $(CF_3P)_4$, 30 min of reflux was required. Prolonged reflux (3 h) was required to achieve extensive reaction of $[Ni(dppe)_2]$ with $(CF_3P)_{4,5}$.

Preparation of $[Pd(\eta^2\text{-}CF_3P{=}PCF_3)(PPh_3)_2]$ (9). A frozen (−195 °C) mixture of $[Pd(PPh_3)_4]$ (73 mg, 0.06 mmol), $(CF_3P)_{4,5}$ (109 mg, 0.55 mmol of 9:1 tetramer/pentamer as "$(CF_3P)_2$"), and toluene (0.5 mL) was allowed to warm to room temperature. Reaction was complete within 5 min. Overnight cooling of the solution to −20 °C yielded a crop of yellow crystals (33 mg) of $[Pd(CF_3P{=}PCF_3)(PPh_3)_2]$ (63%), mp 210–211 °C. Anal. Calcd for $C_{38}H_{30}F_6P_4Pd$: C, 54.91; H, 3.61. Found: C, 54.62; H, 3.74. MW: calcd 830.95, found (in C_6H_6) 785 (830.95 by X-ray crystallography). Mass spectral data (m/e, $[species]^+$ (relative intensity where % of strongest peak = 100): 830, $[M]^+$ (1); 760, $[M - PCF]^+$ (1.4); 630, $[M - (PCF_3)_2]$ (10); 568, $[M - PPh_3]^+$ (1); 500, $(CF_3P)_5^+$ (1.5); 431 $[(CF_3)_4P_5]^+$ (1.8); 400, $(CF_3P)_4^+$ (25); 368, $[Pd(Ph_3P)]^+$ (11); 300,$(CF_3P)_3^+$ (4); 262, $[PPh_3]^+$ (100); 185, $[PPh_2]^+$ (84); 108, $[PPh]^+$ (62); 69, $[CF_3]^+$ (9). Infrared spectrum (1600–400 cm^{-1}): 1478 (s), 1434 (s), 1128, 1113, 1090, 1076 (all vs), 1026 (s), 998 (s), 744 (s–vs), 693 (vs), 530 (s), 517 (s), 503 (s), 490 (s), 447 (w), 435 (w), 417 (w). Single crystals of **9** suitable for X-ray crystallography were grown by slow evaporation of a chloroform solution in air.

Intermetallic Transfer. Adding between 0.5 and 1 equiv of $Pt(\eta^2\text{-}C_2H_4)(PPh_3)_2$ to the Pd complex in $CDCl_3$ at 25 °C resulted in immediate evolution of gas (ethylene) and formed a new species identified as $Pt(Ph_3P)_2Pt(\eta^2\text{-}CF_3PPCF_3)$. This species was identical with that formed directly from Pt(0) complexes and $(CF_3P)_4$ with reflux. The ratio of new Pt complex to **9** was about 1:1, and further addition of a large excess (4 equiv) of $Pt(\eta^2\text{-}C_2H_4)(PPh_3)_2$ did not affect the relative concentrations of the diphosphene complexes.

X-ray Data Collection and Structure Solution[16,17] for $[Pd(\eta^2\text{-}CF_3P{=}PCF_3)(PPh_3)_2]$ (9). A yellow, prismatic crystal of $C_{38}H_{30}F_6P_4Pd$, having approximate dimensions of 0.14 × 0.14 × 0.31 mm, was mounted in a nonspecific orientation on an Enraf-Nonius CAD4 automated diffractometer. All intensity measurements were performed using Mo Kα radiation (λ = 0.71073 Å) with a graphite crystal, incident beam monochromator.

The automatic peak search and reflection indexing programs[18] in conjunction with a cell reduction program showed the crystal to be monoclinic, and from the systematic absences of $h0l$, $h + l$ odd, and $0k0$, k odd, the space group was determined to be $P2_1/n$, an alternative setting of $P2_1/c$ (No. 14).[19] Cell constants were obtained from a least-squares refinement of the setting angles of 24 reflections in the range $15 < 2\theta < 27°$.

The intensity data were collected at room temperature (23 °C) using an ω–2θ scan ranging in speed from 10.1 to 1.2 deg/min (in ω). The variable scan rate was chosen to give $\sigma(I)/I \le 0.02$ within a time limit of 60 s in order to achieve improved counting statistics for both intense and weak reflections in a minimum time. The scan range was determined as a function of θ to compensate for the α_1–α_2 wavelength dispersion: ω

(3) Elmes, P. S.; Scudder, M. L.; West, B. O. *J. Organomet. Chem.* **1976**, *14*, 33.
(4) Jones, R. A.; Seberger, M. H.; Whittlesey, B. R. *J. Am. Chem. Soc.* **1985**, *107*, 6424 and references therein.
(5) Burg, A. B.; Mahler, W. *J. Am. Chem. Soc.* **1958**, *80*, 2334.
(6) Cowley, A. H.; Hill, K. E. *Inorg. Chem.* **1973**, *12*, 1446.
(7) Gatehouse, B. M. *Chem. Commun.* **1969**, 948.
(8) Shriver, D. F. *The Manipulation of Air Sensitive Compounds*; McGraw-Hill Series in Advanced Chemistry; McGraw-Hill: New York, 1969.
(9) Mahler, W.; Burg, A. B. *J. Am. Chem. Soc.* **1958**, *80*, 6161.
(10) Bennett, F. W.; Emelēus, H. J.; Haszeldine, R. N. *J. Chem. Soc.* **1953**, 1565.
(11) Blake, D. M.; Roundhill, D. M. *Inorg. Synth.* **1978**, *18*, 121.
(12) Yoshida, T.; Matsuda, T.; Otsuka, S. *Inorg. Synth.* **1979**, *19*, 110.
(13) Clark, H. C.; Itoh, K. *Inorg. Chem.* **1971**, *10*, 1707.
(14) Hartley, F. R. *Organomet. Chem. Rev. A* **1970**, *6*, 119.
(15) Chatt, J.; Hart, F. A. *J. Chem. Soc.* **1960**, 1398. Chatt, J.; Hart, F. A.; Watson, H. R. *J. Chem. Soc.* **1962**, 2537.

(16) This X-ray crystallographic study comprises report No. SR:030122-06-84 of the Structure Determination Laboratory, Department of Chemistry, University of Alberta.
(17) Complete details of the crystallographic results including all bond lengths, bond angles and torsional angles, anisotropic and equivalent isotropic thermal vibrations, root-mean-square amplitudes of thermal vibrations, and structure factors are available as supplementary material.
(18) The diffractometer programs are those supplied by Enraf-Nonius for operating the CAD4F diffractometer with some local modifications and additions.
(19) *International Tables for X-ray Crystallography*; Kynoch Press: Birmingham, England, 1969; Vol. I.

Table I. Crystallographic Data for **9**

chem formula $C_{38}H_{30}F_6P_4Pd$	space group monoclinic $P2_1/n$
fw 830.95	T = 23 °C
a = 11.200 (2) Å	λ = 0.71073 Å (graphite monochromated)
b = 19.441 (3) Å	ρ_{calc} = 1.479 g cm^{-3}
c = 17.502 (3) Å	$R_1{}^a$ = 0.048
β = 101.71 (1)°	$R_2{}^a$ = 0.062
V = 3732 Å^3	GOF^a = 1.89
Z = 4	

$^a R_1 = \sum||F_o| - |F_c||/\sum|F_o|$; $R_2 = (\sum w(|F_o| - |F_c|)^2/\sum wF_o^2)^{1/2}$; GOF $= [\sum w(|F_o| - |F_c|)^2/(NO - NV)]^{1/2}$.

scan width (deg) = 0.60 + 0.35 tan θ.

Backgrounds for the peaks were measured by extending the scan 25% on either side of the calculated range to give a peak to background counting time of 2:1. Intensity measurements were made out to a maximum 2θ of 54.00°. There were three reflections which were chosen as standard reflections, and these were remeasured every 60 min of exposure time to check on crystal and electronic stability over the course of data collection. A linear regression analysis of these standards showed a mean change in intensity of −8.6 (1.5%) over the time of data collection.

Data Reduction. A total of 8661 reflections were collected. The data were corrected for Lorentz, polarization, and background effects according to the usual formulas. Averaging equivalent forms and rejecting systematically absent data left 8137 unique reflections of which 4322, having $I > 3\sigma(I)$, were used in the structure solution and refinement.

The structure was solved[20] using a three-dimensional Patterson synthesis which gave the positional parameters for the Pd and two P atoms. The remaining non-hydrogen atoms were located by the usual combination of least-squares refinement and difference Fourier synthesis.

Refinement of atomic parameters was carried out by using full-matrix least-squares techniques on F_o minimizing the function $\sum_w(|F_o| - |F_c|)^2$, where $|F_o|$ and $|F_c|$ are the observed and calculated structure factor amplitudes, respectively, and the weighting factor w is given by $w = 4F_o^2/\sigma^2(F_o^2)$. The neutral-atom scattering factors were calculated from the analytical expression for the scattering factor curves.[21] The f' and f'' components of anomalous dispersion[22] were included in the calculations for all non-hydrogen atoms. Contributions from the H atoms were not included in the calculations.

In the final cycle 442 parameters were refined using 4322 observations having $I > 3\sigma(I)$. The final agreement factors were $R_1 = \sum||F_o| - |F_c||/\sum|F_o| = 0.048$ and $R_2 = (\sum w(|F_o| - |F_c|)^2/\sum wF_o^2)^{0.5} = 0.061$. The largest shift in any parameter was 0.03 times its estimated standard deviation, and the error in an observation of unit weight was 1.89 e. An analysis of R_2 in terms of F_o, λ^{-1} sin θ, and various combinations of Miller indices showed no unusual trends. The highest peak in the final difference Fourier was 0.8 (1) e A^{-3}; it is located near the Pd atom and is not chemically significant. Table I lists the crystal data and the details of the intensity collection. The positional (×10^4) and thermal (×10^2) parameters of **9** are given in Table II.

Results

The sole palladium-containing product from the reaction of [Pd(PPh_3)$_4$] and excess *cyclo*-(CF_3P)$_{4,5}$ in toluene at +25 °C was the compound [Pd(η^2-CF_3P=PCF_3)(PPh_3)$_2$] (**9**). Formed completely within 5 min (spectroscopically the yields are quantitative), **9** can be isolated as pale yellow prisms in 60–70% yields. Unreacted (CF_3P)$_{4,5}$ and displaced PPh_3 are the only remaining species detectable in ^{31}P and ^{19}F NMR spectra of typical reaction mixtures. A structural determination (vide infra) confirms that, in common with the product of the reaction of (C_6F_5P)$_4$ with [Pt(PPh_3)$_3$] in refluxing benzene,[3] **9** contains an *E*-configuration diphosphene (CF_3P=PCF_3) "side-on" bonded to a [Pd(PPh_3)$_2$] moiety (Figure 1). In addition **9** has a characteristic ^{19}F NMR spectrum (Figure 2).

Crystal Structure of 9. Details of the structural determination are given in Tables I–III, and the molecular structure is shown in Figure 1 (complete lists of all parameters for **9** are given in

(20) The computer programs used in this analysis include the Enraf-Nonius Structure Determination Package by B. A. Frenz (*Computing in Crystallography*; Delft University Press: Delft, Holland, 1978; pp 64–71) and several locally written or modified programs.
(21) *International Tables of X-ray Crystallography*; Kynoch Press: Birmingham, England, 1974; Vol. IV, Table 2.2B.
(22) Reference 21, Table 2.3.1.

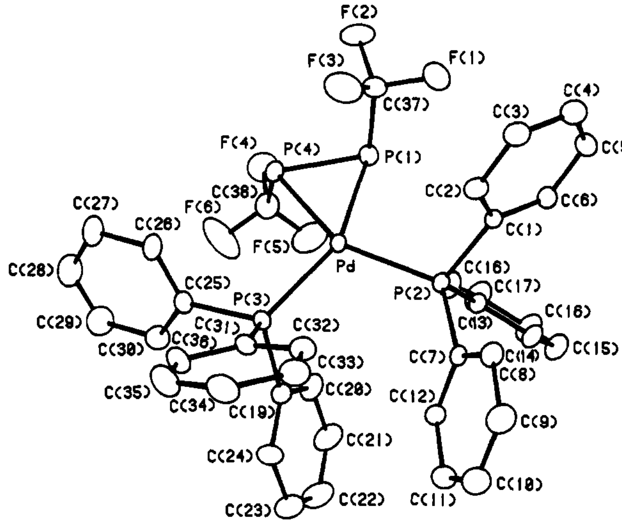

Figure 1. Molecular structure of Pd(η^2-CF_3P=PCF_3)(PPh_3)$_2$ (**9**), showing atom numbering. The atoms are represented by 30% ellipsoids.

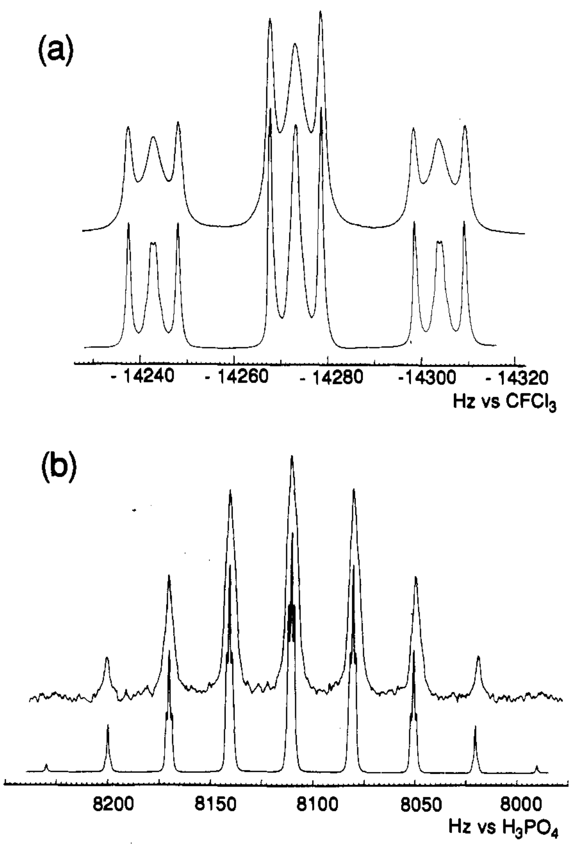

Figure 2. (a) ^{19}F NMR spectrum of **9** at 376.4 MHz in $CDCl_3$ solution and that calculated using coupling constants given in Table V. (b) ^{31}P NMR spectrum of the diphosphene part of **9** at 161.98 MHz in $CDCl_3$ solution also accompanied by a calculated spectrum.

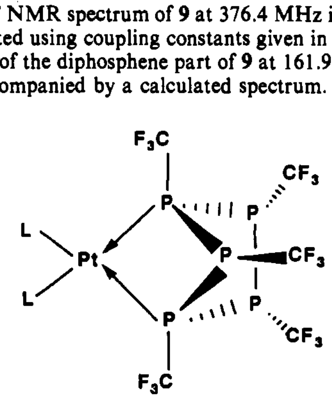

Figure 3. Proposed geometry of **20**[29,32] and by implication **22** and **23**. Similar structures are visualized for **24** (Pd) and **25** (Ni) with dppe in place of Ph_3P groups.

Table II. Positional (×10⁴) and Thermal (×10²) Parameters of **9**

atom	x	y	z	U,ᵃ Å²	atom	x	y	z	U,ᵃ Å²
Pd	443.0 (4)	12.6 (3)	−2223.9 (3)	3.38 (1)	C(15)	5725 (7)	384 (5)	−1894 (5)	6.8 (3)
P(1)	364 (2)	1238.8 (9)	−2189 (1)	4.69 (6)	C(16)	5438 (7)	806 (5)	−2543 (5)	7.7 (3)
P(2)	2401 (1)	−130.0 (8)	−1422.4 (9)	3.46 (5)	C(17)	4208 (7)	952 (5)	−2852 (5)	8.3 (3)
P(3)	−240 (2)	−1047.1 (9)	−2782 (1)	4.14 (5)	C(18)	3281 (6)	640 (4)	−2538 (4)	5.9 (3)
P(4)	−1155 (2)	712.8 (9)	−2856 (1)	4.92 (6)	C(19)	873 (6)	−1432 (4)	−3282 (4)	5.1 (2)
F(1)	512 (5)	1628 (3)	−720 (3)	9.8 (2)	C(20)	1590 (6)	−981 (5)	−3640 (4)	6.4 (3)
F(2)	−1050 (5)	2021 (2)	−1491 (3)	10.2 (2)	C(21)	2493 (8)	−1246 (5)	−4004 (4)	8.3 (3)
F(3)	−1035 (5)	922 (3)	−1104 (3)	11.0 (2)	C(22)	2693 (8)	−1949 (5)	−3995 (5)	9.6 (4)
F(4)	−1089 (5)	1475 (3)	−4124 (3)	10.2 (2)	C(23)	2017 (8)	−2392 (5)	−3646 (5)	9.3 (4)
F(5)	444 (5)	854 (3)	−3863 (3)	12.2 (2)	C(24)	1091 (7)	−2140 (4)	−3269 (5)	7.4 (3)
F(6)	−1249 (8)	402 (3)	−4345 (3)	15.8 (3)	C(25)	−1634 (6)	−1018 (4)	−3529 (4)	5.7 (2)
C(1)	2508 (5)	356 (3)	−520 (3)	3.5 (2)	C(26)	−2692 (7)	−771 (4)	−3296 (5)	7.1 (3)
C(2)	1681 (6)	194 (3)	−46 (4)	4.8 (2)	C(27)	−3800 (8)	−726 (5)	−3852 (6)	10.2 (4)
C(3)	1701 (7)	553 (4)	649 (4)	5.6 (2)	C(28)	−3802 (9)	−924 (6)	−4628 (7)	13.2 (5)
C(4)	2541 (7)	1086 (4)	867 (4)	6.1 (3)	C(29)	−2783 (9)	−1166 (6)	−4837 (6)	11.9 (4)
C(5)	3353 (6)	1265 (4)	385 (4)	5.9 (3)	C(30)	−1654 (8)	−1205 (5)	−4291 (5)	8.7 (3)
C(6)	3361 (6)	890 (3)	−310 (4)	4.9 (2)	C(31)	−573 (6)	−1724 (3)	−2136 (4)	4.8 (2)
C(7)	3017 (5)	−979 (3)	−1098 (4)	3.8 (2)	C(32)	185 (6)	−1782 (4)	−1397 (4)	5.4 (2)
C(8)	3159 (6)	−1198 (3)	−326 (4)	5.0 (2)	C(33)	−15 (7)	−2309 (4)	−877 (4)	6.3 (3)
C(9)	3546 (7)	−1878 (4)	−129 (5)	6.9 (3)	C(34)	−1005 (8)	−2752 (4)	−1090 (5)	7.2 (3)
C(10)	3804 (7)	−2320 (4)	−679 (5)	6.7 (3)	C(35)	−1769 (8)	−2675 (4)	−1822 (5)	8.1 (3)
C(11)	3702 (7)	−2098 (4)	−1467 (5)	6.5 (3)	C(36)	−1564 (7)	−2175 (4)	−2361 (5)	6.8 (3)
C(12)	3283 (6)	−1426 (3)	−1666 (4)	5.2 (2)	C(37)	−357 (7)	1458 (4)	−1351 (4)	5.9 (3)
C(13)	3598 (5)	224 (3)	−1874 (4)	4.0 (2)	C(38)	−735 (8)	860 (4)	−3830 (5)	7.3 (3)
C(14)	4830 (6)	92 (4)	−1567 (4)	5.2 (2)					

ᵃ All atoms were refined anisotropically. The equivalent isotropic thermal parameter is given by $U = {}^1/_3(U_{11} + U_{22} + U_{33} + 2U_{23}\cos\alpha + 2U_{13}\cos\beta + 2U_{12}\cos\gamma$.

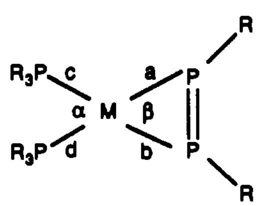

Figure 4. Important bond angles and lengths for the system delineated in Table IV.

the supplementary material). Comparative structural results are given in Table IV.

The central core of compound **9** defined by the Pd and the four phosphorus nuclei of the Ph_3P and $CF_3P{=}PCF_3$ groups is very nearly planar. There is a 9° dihedral angle between the two [PdP_2] planes (Pd(*P*Ph_3)$_2$ or Pd(CF_3*P*=*P*CF_3)) of **9**. The distortion from planarity is greater in **9** than in **3** (3°)[2] (or in the related complexed species (dppe)Pd(η^2-PhPPPh)(W(CO)$_5$)$_2$ (**10**) (3°)[2]), but the distortion is not as pronounced as that shown by **4** (20.4°).[3] The increased distortion displayed by both Ph_3P complexes **9** and **4** relative to the dppe analogues **3** and **10** is most likely due to the fact that the dppe ligand is a chelate with a smaller bite angle at phosphorus (87° [2]) compared to 108° [3] for the angle developed between two independent Ph_3P ligands. This larger steric requirement of the two independent Ph_3P groups is relieved by distorting the η^2-diphosphene out of the square plane. A comparison of the relative distortions shown by **4** and **9** suggests that the increased steric bulk of the C_6F_5 substituents in **4**[3] also contributes to the distortion observed there. P=P bond lengths are comparable for **3**, **4**, **9**, and (Et_3P)$_2$Ni($Me_3SiPPSiMe_3$) (**11**).[23]

NMR Spectroscopy of the η^2-Diphosphene Complex 9. The $^{31}P\{^{19}F\}$ spectrum of **9** (Figure 2a) is typical of an AA′XX′ [24] spin system. The splitting due to $|^1J_{PP}|$ for the diphosphene phosphorus is at least 300 Hz. Selective diphosphene or tertiary phosphine phosphorus-decoupled ^{19}F NMR experiments show that the complex ^{19}F signal of Figure 2a is reduced to a 1:2:1 triplet of complex multiplets. The diphosphene phosphorus-decoupled fluorine spectrum did not show the same line shape as the individual pseudotriplets. The spin system is therefore more correctly labeled as [X_3AM]$_2$. This system meets the condition $|J_{AA'}| \gg |J_{AX} + J_{AX'}|$[24] and $|^4J_{F,P}(\text{"cis"}) + {}^4J_{F,P}(\text{"trans"})|$ is 10.7 Hz. The ^{31}P NMR spectrum of the diphosphene phosphorus atoms of **9** (Figure 2b) shows clearly the central seven lines of a nine-line pattern. The Ph_3P portion of **9** (not shown) is a "triplet" broadened by small, long-range coupling to fluorine. The separation of the outer lines the triplet (62 Hz) is the splitting $|^2J_{PP}(\text{trans}) + {}^2J_{PP}(\text{cis})|$,[2,24] which is also observed in the $^{31}P\{^{19}F\}$ spectrum. The calculated (NUMARIT[25]) second-order patterns are shown in Figure 2. Despite repeated attempts using either $X_3AA'X_3'$ or [X_3AM]$_2$ descriptions we were unable to completely determine all coupling constants because the experimental line widths were too broad.

Table III. Selected Bond Distances and Bond Angles in **9**ᵃ

	Bond Distances (Å)		
Pd–P(1)	2.387 (1)	P(3)–C(19)	1.822 (5)
Pd–P(2)	2.367 (1)	P(3)–C(25)	1.822 (5)
Pd–P(3)	2.341 (1)	P(3)–C(31)	1.823 (5)
Pd–P(4)	2.340 (1)	F(1)–C(37)	1.357 (6)
P(1)–P(4)	2.121 (2)	F(2)–C(37)	1.334 (6)
P(1)–C(37)	1.861 (6)	F(3)–C(37)	1.311 (7)
P(4)–C(38)	1.880 (7)	F(4)–C(38)	1.330 (7)
P(2)–C(1)	1.823 (5)	F(5)–C(38)	1.332 (8)
P(2)–C(7)	1.834 (5)	F(6)–C(38)	1.314 (8)
P(2)–C(13)	1.825 (5)	C–C(av)ᵇ	1.40 (5)
	Bond Angles (deg)		
P(1)–Pd–P(2)	97.85 (4)	Pd–P(2)–C(7)	122.3 (1)
P(1)–Pd–P(3)	151.51 (5)	Pd–P(2)–C(13)	111.9 (2)
P(1)–Pd–P(4)	53.30 (5)	Pd–P(3)–C(19)	111.4 (2)
P(2)–Pd–P(3)	109.22 (4)	Pd–P(3)–C(25)	115.6 (2)
P(2)–Pd–P(4)	151.15 (5)	Pd–P(3)–C(31)	117.8 (2)
P(3)–Pd–P(4)	99.24 (5)	P(1)–C(37)–F(1)	110.0 (4)
Pd–P(1)–P(4)	62.23 (5)	P(1)–C(37)–F(2)	111.9 (4)
Pd–P(4)–P(1)	64.47 (5)	P(1)–C(37)–F(3)	118.3 (4)
Pd–P(4)–C(38)	102.1 (2)	P(4)–C(38)–F(5)	118.0 (5)
Pd–P(1)–C(37)	105.9 (2)	P(4)–C(38)–F(6)	111.2 (5)
P(4)–P(1)–C(37)	96.7 (2)	P(4)–C(38)–F(4)	112.2 (5)
P(1)–P(4)–C(38)	96.0 (2)	F–C–F(av)ᶜ	105.0 (14)
Pd–P(2)–C(1)	110.1 (1)	C–C–C(av)ᵈ	120 (3)

ᵃ Numbers in parentheses are estimated standard deviations in the least significant digits. ᵇ Average C–C distance in phenyl rings of PPh_3 groups. ᶜ F–C–F bond angles in CF_3 groups. ᵈ Phenyl ring internal bond angles in PPh_3 groups.

(23) Deppisch, B.; Schafer, H. *Acta Crystallogr.* **1982**, *B38*, 748.
(24) Harris, R. K. *Can. J. Chem.* **1964**, *42*, 2275.
(25) Personal communication from J. S. Martin (University of Alberta) and K. Worvil (University of East Anglia).

Table IV. Comparative Structural Parameters on η^2-RP=PR Complexes of Ni, Pd, and Pt[a,b]

compd	d(P=P), Å	α, deg	β, deg	a, b, Å	c, d, Å	C–P=P–C	C–P–P–C	twist, deg	ref
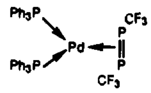 9	2.121 (2)	109.22 (4)	53.30 (5)	2.387 (1) 2.340 (1)	2.367 (1) 2.341 (1)	96.0 (2) 96.7 (2)	155.0	9	c
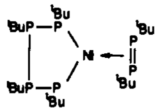 6	2.110 (5)	101.5	55.8	2.255	2.149		160.5	0	4
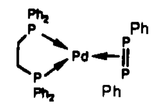 3	2.121 (4)	86.7 (1)	53.3 (1)	2.366 (2)	2.304 (2)	101.9 (3)	163	3	2
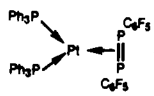 4	2.156 (7)	107.0 (2)	54.8 (2)	2.364 (5) 2.319 (5)	2.349 (5) 2.329 (4)	102.0 (6) 104.1 (6)		20.4	3
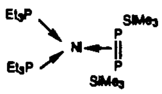 11	2.148 (2)	104.55 (5)	57.13 (5)	2.58 (2) 2.236 (2)	2.179 (2) 2.175 (2)	96.96 (8) 97.87 (8)			23
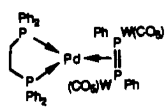 10	2.186 (6)	84.7 (2)	55.1 (2)	2.375 (4) 2.355 (4)	2.305 (4) 2.307 (6)	103.8 (6) 105.7 (6)	156	3	2

[a] Angles α and β and bond lengths a–d are illustrated in Figure 4. [b] The "twist" is the dihedral angle between the [$M(PR_3)_2$] and the [M–$(PR)_2$] planes. [c] This work.

Table V. NMR Spectroscopic Parameters[a] of the Diphosphene Complexes **9** and **12–16**

	δ(P), ppm	$\lvert ^2J_{P,P}$(cis) + $^2J_{P,P}$(trans)$\rvert$[b]	$^1J_{P,Pt}$	δ(P), ppm	$J_{P,Pt}$	$\lvert ^2J_{P,F} + {}^3J_{P,F}\rvert$[c]	$\lvert ^4J_{P,F}$(cis) + $^4J_{P,F}$(trans)$\rvert$[d]	$J_{F,Pt}$	δ(F), ppm
9	+50.5 (i)	62.4		+22.7		60.2	10.7		−37.20
12	+19.5 (i)	67.1	3248.1	−28.0	251.0	58.7	6.0	87.3	−35.60
13			e			58.5	12.5	83.0	−39.31
14	+20.0 (ii)	70.1	3347.1	−6.2	356.0	59.4	11.3	89.7	−38.40
15	46.33	70.9		19.57		63.2	14.2		−42.78
16	+44.95	56.7		+12.42		63.2	8.32		−38.70

[a] Recorded in (i) toluene-d_8 or (ii) benzene-d_6 at +25 °C. J values are given in Hz. [b] Defined as for an AA'XX' spin system. [c] This is the separation between the strong outer lines of the X part of the [X_3AM]$_2$ pseudotriplet. [d] Estimated from the separations of the strong outer lines of the doublet or pseudotriplet satellites of [X_3AM]$_2$ pseudotriplet of pseudotriplets (or doublets). [e] ^{31}P signals of this species were not unambiguously identified in spectra owing, we think, to rapid exchange of free and ligated PMe_2Ph.

We have used a smaller but reasonable line width for the calculated spectra to show the expected general form arising from the major coupling constants.

Reactions of Polyphosphines with Zerovalent Platinum Group Metal Complexes: Final Products. When toluene or benzene solutions of (CF_3P)$_{4,5}$ (2 equiv excess as $CF_3P{=}PCF_3$) and [ML_n] (M = Pt, n = 3, L_3 = (η^2-C_2H_4)(PPh_3), L = PEt_3; M = Pt, n = 4, L = PEt_3, PMe_2Ph, PPh_3; M = Pd, Ni, n = 2, L = $Ph_2PCH_2CH_2PPh_2$ (dppe) (1 equiv)) are refluxed for between 10 min and 3 h, the major product in every case is a diphosphene complex [M(η^2-$CF_3P{=}PCF_3$)L_2] (M = Pt, L = PEt_3 (**12**), PMe_2Ph (**13**), PPh_3 (**14**); M = Pd (**15**), Ni (**16**), L = dppe). These have been identified by ^{31}P and ^{19}F NMR spectroscopy (Table V). The assignments are based on close similarities of the ^{31}P and ^{19}F NMR signal patterns of these species to those of the structurally characterized Pd complex **9** (vide supra). Furthermore, the characteristically small phosphorus–platinum-195 splittings of 250–350 Hz, evident in complexes of that metal, compare most favorably to values previously measured for the diphosphene phosphorus in the complexes Pt(η^2-PhP=PPh)L_2 (L = PPh_3 (**2**), L_2 = dppe (**3**)).[2] Such small P–Pt coupling constants are typical for π-bound P–P and P–C multiple bonds bound to zerovalent platinum.[2,26] The ^{31}P{^{19}F} NMR spectrum of **9**, like the ^{31}P NMR spectra of **2** and **3**,[2] is characteristic for an AA'XX' nuclear spin system.[24] High-field ^{19}F and ^{31}P NMR spectra of the reaction mixtures also show complex resonances in low concentration of what we believe to be other (cyclopolyphosphine)-metal complexes. These will be discussed below.

NMR Spectroscopy of η^2-Diphosphene Complexes 12–16. The relative simplicity of the fluorine NMR spectra of **12** and **14**, which appear as triplets of doublets split by coupling to ^{195}Pt, probably arises because both the long-range tertiary phosphine–phosphorus coupling (either $^4J_{FP}$("cis") or $^4J_{F,P}$("trans")) and phosphorus–phosphorus coupling between the cis-disposed tertiary phosphines are negligible. Although ^{19}F spectra of **13** are broadened, the spectral features are similar to those of the related complexes. Likewise ^{19}F NMR spectra of (dppe)Ni(η^2-CF_3PPCF_3) (**16**) appear as 1:2:1 triplets of 1:2:1 triplets. The spectra of (dppe)Pd(η^2-$CF_3P{=}PCF_3$) (**15**) are essentially identical in line shape to those of **9** but differ significantly in shifts and in the magnitudes of the coupling constants (Table V).

This regular progression of the character of the Pt, Pd, and Ni ^{19}F NMR spectra from 1:2:1 triplets of doublets to 1:2:1 triplets of pseudotriplets to 1:2:1 triplets of 1:2:1 triplets most likely reflects large changes in the values for phosphorus–phosphorus coupling between the cis-disposed tertiary phosphine nuclei of the complexes. A comprehensive study[27] of divalent Ni, Pd, and Pt

(26) Kraaijkamp, J. G.; van-Koten, G.; van der Knaap, T. A.; Bickelhaupt, F.; Stam, C. H. *Organometallics* **1986**, *5*, 2014. Burckett St. Laurent, J. C. T. R.; Hitchcock, P. B.; Kroto, H. W.; Nixon, J. F. *J. Chem. Soc., Chem. Commun.* **1981**, 1141.

(27) Charrier, C.; Maigrot, N.; Mathey, F.; Robert, F.; Jeannin, Y. *Organometallics* **1986**, *5*, 623.

Table VI. ^{19}F NMR Spectroscopic Parameters (J in Hz) of the Pentamer Complexes **20** and **22–25**

M	L		F	δ(F), ppm	$^2J_{F,P}$	$\|^2J_{F,P} + {}^3J_{F,P}\|$	$^3J_{F,P}$	$J_{F,Pt}$
Pt	PEt_3	**22**	F_A[a]	−40.57	36.0		25.4, 10.0	94.0
			F_B[b]	−38.59		59.5	12.0	85.7
			F_C[d]	−57.75	50.6		12.7	0
Pt	PMe_2Ph	**23**	F_A	−40.42	35.7		26.1, 11.3	96.1
			F_B	−38.10		58.6	12.3	82.8
			F_C	−57.42	51.0		12.1	0
Pt	PPh_3	**20**	F_A	−40.97	36.0		25.9, 10.1	94.2
			F_B	−38.27		59.2	11.8	89.0
			F_C	−56.73	51.3		10.1	0
Pd	L_2 = dppe	**24**	F_A	−39.40	31.8		22.0, 9.18	
			F_B	−38.26		*c*		
			F_C	−59.14	50.7		8.2	
Ni	L_2 = dppe	**25**	F_A	−39.09	32.7		24.7, 8.0	
			F_B	−43.49		43.8	11.4	
			F_C	−58.35	48.3		7.5	

[a] All F_A groups resonate as three sets of overlapping doublets. [b] All F_B groups resonate as an $X_3AA'X_3'$ "virtual" 1:2:1 triplet of doublets except as noted. [c] This F signal shows only a broad doublet of splitting of 27 Hz with a signal line width ca. 41 Hz. [d] All F_C signals are first-order doublets of triplets.

complexes of unsymmetric bis(phosphano)ethenes illustrates a similar strong trend of $^2J_{PP}$ with values ca. 70, ca. 40, and <10 Hz, respectively.

Intermediates in Reactions of $(CF_3P)_{4,5}$ with Zerovalent Pt Complexes. (a) Tetramer Reagent $(CF_3P)_4$. There is evidence that other cyclopolyphosphine complexes occur during reaction of $(CF_3P)_4$ with $[Pt(\eta^2\text{-}C_2H_4)(PPh_3)_2]$ or $[PtL_n]$ (n = 3, L = PEt_3; n = 4, L = PEt_3, PMe_2Ph, PPh_3) in toluene at +25 °C. These species may have bearing on the reaction pathway. Ethylene is completely displaced from the Pt–ethylene complex. The ^{31}P NMR spectra of these reaction mixtures showed complex multiplets, but the signals were not readily interpretable. In every case however ^{19}F NMR spectra at +25 °C were characterized by two pronounced broad resonances near −41.0 ppm ($\Delta\nu_{1/2}$ 250–300 Hz) and −52.7 ppm ($\Delta\nu_{1/2}$ 350–400 Hz) of equal intensity. Cooling to −50 °C separates the broad signals into two distinct sets of ^{19}F resonances in the intensity ratio 2.1:1.

The case of $Pt(\eta^2\text{-}C_2H_4)(PPh_3)_2$ with $(CF_3P)_4$ is typical and illustrative. In this case most of the fluorine signal intensity (68%) consisted of two signal groups of equal integration (δ(F) −39.60 ppm, doublet, J = 23.4 Hz, $J_{F,Pt}$ = 120 Hz, and δ(F) −50.36 ppm, doublet of doublets, J = 33.6 and 16.9 Hz, $J_{F,Pt}$ = 0 Hz). The remaining ^{19}F signal intensity (32%) comprises four signals of equal intensity: two broad triplets δ(F) −35.24 ppm (J = 37.8, $J_{F,Pt}$ = 90 Hz) and δ(F) −38.59 ppm (J = 45.0 Hz, $J_{F,Pt}$ = 102 Hz), a doublet δ(F) −47.24 ppm ($^2J_{F,P}$ = 48.2 Hz), and a multiplet at δ(F) −57.6 ppm. It is clear that in both sets of data that those ^{19}F signals which are split by coupling to platinum-195 resonate with shifts and splittings similar to (but not identical with) the fluorine signals of $[Pt(\eta^2\text{-}CF_3P{=}PCF_3)(PPh_3)_2]$ (δ(F) −36.44 ppm, $J_{F,Pt}$ = 89.7 Hz). The more shielded resonances in both sets of data are similar to (but not identical with) the fluorine shift of $(CF_3P)_4$ (δ(F) −51.25 ppm). At reflux temperatures these signals disappear within 20 min and signals due to $[Pt(\eta^2\text{-}CF_3P{=}PCF_3)(PPh_3)_2]$ and "pentamer" complexes (see below) are observed. We suggest that both these sets of intermediate resonances observed in ^{19}F NMR spectra correspond to two species of the same composition, namely $[Pt\{(CF_3P)_4\}\cdot(PPh_3)_2]$, which are in dynamic equilibrium at +25 °C. An equilibrium (eq 6) between

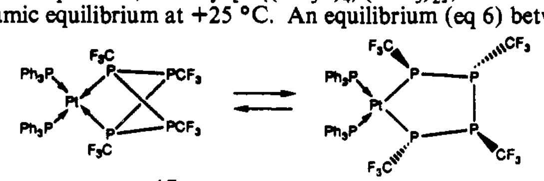

17a **17b** (6)

a 1,3-dicoordinated $(PCF_3)_4$–Pt complex **17a** and a $\overline{Pt(PCF_3)_3PCF_3}$ metallacycle **17b** (cf. **6**) would be consistent with the patterns displayed by the two sets of ^{19}F NMR signals, and the individual peaks in each pattern observed at −50 °C can be reasonably assigned to the CF_3 signals which would be expected for the two forms of **17**. The metallacycle **17b** is not without precedent in that a similar structure has been observed in **6**.[4] In that case the $Ni(Bu^tP)_4$ ring was strictly planar.[4] The multiplicity of fluorine signals arising from **17b** leads us to suspect that the ring is not planar in this metallacycle perhaps because the Ph_3P ligands have more steric bulk than the $(Bu^tP)_2$ unit in **6** and interference with the CF_3 groups distorts the ring. Comparable species (**18a,b**, L = PEt_3; **19a,b**, L = PMe_2Ph) can be proposed for the other two phosphine ligands. It is significant that if the solutions containing these signals (initially representing about 90% of the total fluorine intensity) were maintained at +25 °C for periods approaching 2 weeks, all traces of the species involved in the putative equilibria were replaced by the pentamer complexes (**20**, **22**, and **23**, respectively (vide infra)) long before the corresponding η^2-diphosphene complexes (**14**, **12**, and **13**, respectively) were observed. These tetramer equilibria were not observed during the reactions of $[M(dppe)_2]$ (M = Pd, Ni) with $(CF_3P)_{4,5}$ (9:1 tetramer/pentamer). In both of these cases reaction proceeds to give mixtures of only **15** and **16**, the $\eta^2\text{-}CF_3PPCF_3$ complexes as major products, and **24** and **25**, the pentamer complexes, as minor products, respectively. Without aid of reflux **24** appears first after 1 day in the Pd example followed by **15** after approximately 1-week duration. However, where M = Ni, reaction did not occur at room temperature.

(b) Pentamer Reagent $(CF_3P)_5$. In the reaction of enriched samples of $(CF_3P)_5$ with $[Pt(\eta^2\text{-}C_2H_4)(PPh_3)_2]$ at room temperature, complete displacement of ethylene (^1H NMR spectroscopy) occurred to give a single species that was identical to the minor product obtained from refluxing benzene solutions of $[Pt(\eta^2\text{-}C_2H_4)(PPh_3)_2]$ and excess $(CF_3P)_{4,5}$ (9:1 tetramer/pentamer). Moreover, this species is conspicuously absent from the reaction of pure $(CF_3P)_4$ with $[Pt(\eta^2\text{-}C_2H_4)(PPh_3)_2]$ in toluene at +25 °C, where a completely different reaction (at least initially) occurs, as discussed above. Despite repeated attempts with all of the metal systems investigated herein, no sample of this new species could be isolated because of the ready transformation to the η^2-diphosphene compounds. These diphosphene complexes themselves proved difficult to isolate pure; accordingly, only spectroscopic evidence (Table VI) is available for characterization. The $[Pt(PPh_3)_2]$ example discussed below is representative of the NMR spectral behavior of these species. Similar features were observed in reactions of the other tertiary phosphine metal complexes with mixed cyclopolyphosphines $(CF_3P)_{4,5}$.

Of the four phosphorus NMR signals which appear in the intensity ratio 2:2:2:1 in order of decreasing ^{31}P NMR frequency (labeled P_a, P_b, P_c, and P_d, respectively), only the two most deshielded phosphorus nuclei, P_a and P_b, are bound directly to platinum as evidenced by $^1J_{P,Pt}$ values of 3400 and 2500 Hz, respectively. The latter signal, P_b, is broadened extensively in ^1H-coupled spectra and not significantly coupled to ^{19}F, and so the P_b signal is assigned to the Ph_3P substituents. The large downfield shift is consistent with coordination of tertiary phosphorus to a transition metal.[28] The Ph$_3$P resonance is a doublet which has been assigned as an AA'XX'[2,24] spin system with the major splitting $N = |^2J_{P(Ph_3P),P(PCF_3)}(cis) + {}^2J_{P(Ph_3P),P(PCF_3)}(trans)|$ = 85.4 Hz. All the other phosphorus resonances are complex multiplets split extensively by phosphorus–fluorine and phosphorus–phosphorus interaction.

There are three fluorine environments (as CF$_3$P) with a relative intensity ratio of 2:2:1 in order of decreasing ^{19}F NMR frequency (labeled F$_A$, F$_B$, and F$_C$, respectively). Selective ^{31}P{^{19}F}, ^{19}F{^{31}P}, and ^{31}P{^{31}P} NMR decoupling experiments establish unequivocally the relationship of P$_a$, P$_d$, and P$_c$ with F$_A$, F$_B$, and F$_C$, respectively, and demonstrate clearly that there is no observable ^{19}F–^{19}F coupling.

The most shielded ^{19}F NMR signal F$_C$ (a doublet of triplets due to a $^2J_{P,F}$ and two $^3J_{P,F}$ splittings) belongs to a unique PCF$_3$ group (P$_d$, a triplet of multiplets) which is flanked by two PCF$_3$ groups containing P$_a$ and F$_b$, indicating the existence of a (CF$_3^B$)P$_a$–P$_d$(CF$_3^C$)–P$_a$(CF$_3^B$) subunit. F$_A$ resonates as a 1:2:1 triplet of doublets which reduced to a doublet upon decoupling P$_c$ or a triplet upon decoupling P$_a$. This suggests that F$_A$ and P$_c$ compromise the X and A parts respectively of an X$_3$AA'X$_3$'[24] spin system where $|J_{AA'}|$ is very large with respect to $L = |J_{AX} - J_{AX'}|$, and this produces a "virtual" 1:2:1 triplet. A long-range coupling of F$_a$ to P$_a$($^3J_{F_AP_a}$) of ~10 Hz splits this group into doublets thus suggesting the substructure P$_a$–P$_c$(CF$_3^A$)–P$_c$(CF$_3^A$)–P$_a$. Since the P$_a$ atoms are directly bound to P$_d$ and to ^{195}Pt,[28] it appears that the species is formed of a five-membered phosphorus ring 1,3-dicoordinated to a Pt(Ph$_3$P)$_2$ moiety (a "pentamer" complex), structure **20**.

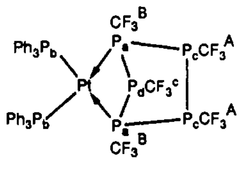

20

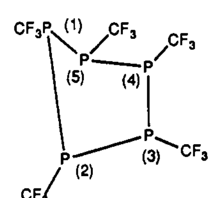

21

The ^{19}F NMR spectrum of the pentamer complex (**20**) will necessarily be complex if, as is likely, the complex is formed by coordination of the P(2) and P(5) phosphorus lone pairs of (CF$_3$P)$_5$ (**21**) (using the designations defined in the crystallographic study of Spencer and Lipscomb[29]). Similar 1,3-coordination of cyclopolyphosphines has been demonstrated crystallographically.[30] This pentamer complex is not stable; solutions of **20**, (CF$_3$P)$_4$, and the η^2-diphosphene complex **14** gradually transformed, on standing at 25 °C, to mixtures of (CF$_3$P)$_{4,5}$ and **14** only.

Similar pentamer complexes [M{(CF$_3$P)$_5$}L$_2$] (M = Pt, L = PEt$_3$ (**22**), PMe$_2$Ph (**23**); M = Pd, L = dppe (**24**); M = Ni, L = dppe (**25**)) are formed. These complexes, with time, decomposed almost entirely to the corresponding η^2-diphosphene species **12**, **13**, and **15** and (CF$_3$P)$_{4,5}$ except for **25**, where decomposition to dppe and unknown precipitates was evident.

Reaction of 9 with Platinum(0) Complexes. We have also observed an interesting reaction between the diphosphene in **9** and a zerovalent Pt complex. Reaction of **9** with the zerovalent platinum substrate [Pt(η^2-C$_2$H$_4$)(PPh$_3$)$_2$] gave **14** as the only new CF$_3$P=PCF$_3$ complex as determined by ^{19}F and ^{31}P NMR spectroscopy (eq 7). The precise nature of the displaced Pd

$$\mathbf{9} + n[\mathrm{Pt}(\eta^2\text{-}\mathrm{C_2H_4})(\mathrm{PPh_3})_2] \rightarrow (1-n)\mathbf{9} + \mathbf{14} + (1-n)\text{``}[\mathrm{Pd}(\mathrm{PPh_3})_2]\text{''} \quad (7)$$

substrate is unknown, and there are no precipitates. When excess [Pt(η^2-C$_2$H$_4$)(PPh$_3$)$_2$] (approximately 4 equiv) was added, **14** remained unaffected.

(28) Nixon, J. F.; Pidcock, A. *Annu. Rev. NMR Spectrosc.* **1969**, *2*, 345.
(29) Spencer, C. J.; Lipscomb, W. N. *Acta Crystallogr.* **1961**, *14*, 250; **1962**, *15*, 509 (corr).
(30) Elmes, P. S.; Gatehouse, B. M.; West, B. O. *J. Organomet. Chem.* **1974**, *84*, 235. Bush, M. A.; Woodward, P. *J. Chem. Soc. A* **1968**, 1221.

Scheme I

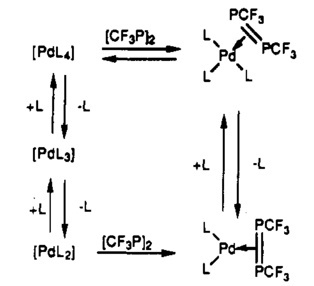

Discussion

Crystal Structure of 9. The P(1)–P(4) bond length of **9** (2.121 (2) Å) is identical to that of **3** (2.121 (4) Å)[2] and slightly longer than that in **6** (2.110 (5) Å) (Table IV). All are shorter than those reported for other mononuclear η^2-diphosphene complexes (2.146 (3)–2.156 (7) Å).[4] Furthermore, the P(1)–P(4) bond is intermediate in length between the double bonds of diphosphenes (2.004 (6)–2.034 (2) Å)[31] and the single bonds of *cyclo*-(CF$_3$P)$_4$ (2.213 (5) Å)[32] or *cyclo*-(CF$_3$P)$_5$ (2.217 (7)–2.257 (7) Å, average 2.223 (7) Å).[29] The C—P=P—C torsional angle of the diphosphene moiety of **9** (155°) suggests a degree of perturbation of the idealized planar P=P π-bond upon coordination that lies midway in the range given by **3** (163°)[2] and **11** (147.7).[23] It is difficult however to assess how much this angle is influenced by the steric bulk of the PPh$_3$ substituents, the electronegativity of the CF$_3$ substituents, and the metal–diphosphene phosphorus distances. In free diphosphenes the C=P=P—C torsional angles are close to 180° (172.2–180.0°), while in the diphosphetene CF$_3$PCF$_3$PC(SiMe$_3$)=C(SiMe$_3$)[33] this is only a little smaller (148.23°) than in **9**.

Synthesis and Reaction Pathways. The synthesis of **9** could be logically considered as the product of rapid reaction between [Pd(PPh$_3$)$_4$] in one or other, or both, of its more reactive dissociated forms [Pd(PPh$_3$)$_n$] (n = 2, 3)[34] with *trans*-CF$_3$P=PCF$_3$ (Scheme I). The latter could be present in trace amounts from the proposed equilibrium (eq 8), which lies far to the left. A

$$[(\mathrm{CF_3P})_4 \rightleftharpoons 2[\mathrm{CF_3P{=}PCF_3}] \quad (8)$$

parallel rationale has been invoked to describe the synthesis and structure of diphosphetenes,[35] and Grobe et al. have trapped CF$_3$P=PCF$_3$ as a Diels–Alder adduct **10** from the in situ reduction of CF$_3$PI$_2$ in the presence of cyclohexadiene in THF[36] (eq 9). This

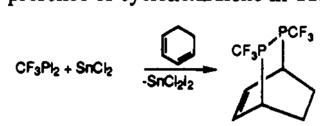

(9)

attractive and simple mechanism does, however, present certain problems. Discrete *trans*-CF$_3$P=PCF$_3$ has neither been isolated nor observed spectroscopically, while recent evidence about diphosphenes[35] would suggest that trifluoromethyl substituents do not have sufficient bulk to prevent dimerization. Though an equilibrium as suggested by eq 8 may be prevalent at elevated temperatures, we suggest that the intermediate or transient products observed in reactions of (CF$_3$P)$_{4,5}$ with a wide variety of zerovalent Ni, Pd, and Pt tertiary phosphine complexes suggests that alternate pathways may be more likely.

It has long been known that (CF$_3$P)$_5$ exists in an equilibrium with (CF$_3$P)$_4$, which is slow to establish itself at +25 °C for neat reactants[9] but which is rapid in the presence of certain nucleophiles

(31) Cowley, A. H. *Acc. Chem. Res.* **1984**, *17*, 386.
(32) Palenik, G. J.; Donahue, J. *Acta Crystallogr.* **1962**, *15*, 564.
(33) Phillips, I. G.; Ball, R. G.; Cavell, R. G. *Inorg. Chem.* **1988**, *27*, 2269.
(34) Ugo, R. *Coord. Chem. Rev.* **1968**, *3*, 319.
(35) Cowley, A. H. *Polyhedron* **1984**, *3*, 389.
(36) Grobe, J.; LeVan, D.; Schulze, J. *Proceedings of the 10th International Conference on Phosphorus Chemistry*, Bonn, FRG, 1986. *Phosphorus Sulphur* **1987**, *30*, 773.

(NMe_3 or PMe_3)[37] and at elevated temperatures.[38] Thus, pure samples of the tetramer, given time (typically days), become contaminated with the pentamer and vice versa. We propose that $(CF_3P)_5$ produced in this way and present initially in undetectably low concentrations readily displaces 1,3-dicoordinated $(CF_3P)_4$ from platinum to give the more stable pentamer complex. This increased stability of the "pentamer" over the "tetramer" complexes probably reflects a reduced degree of ring strain with chelation for the pentamer than might be expected for the tetramer (eq 10).

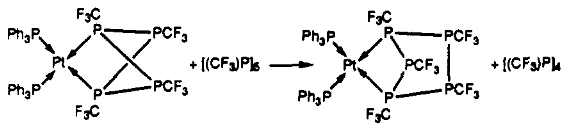
(10)

17a **20**

A previous attempt in this laboratory to stabilize such 1,3-coordinated cyclopolyphosphanes with respect to subsequent ring scission was made using the triphospholene $CF_3PCF_3PCF_3PC(CF_3)=C(CF_3)$. However, the planarity of the heterocycle and the π-acidity of the C=C bond favored olefin rather than phosphorus coordination.[39]

During the reactions of the Pt(0) complexes at 25 °C the η^2-diphosphene complexes are observed only after all traces of the species involved in the dynamic equilibria involving the tetrameric phosphorus species have been transformed to the pentamer-based species. This observation disfavors, at least for Pt, a mechanism where ring scission occurs at the metallacycle stage (eq 11), that

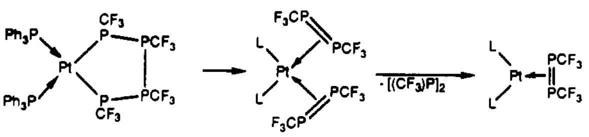
17b **14**

(11)

is, the reverse of the pathway proposed for the formation of **6**. The η^2-diphosphene metal complexes **12–14** seem instead to result from a necessarily more complex ring scission of the pentamer complexes **20** and **22–23**. We suspect also that decomposition occurs by a process similar to that of eq 11, i.e., that the L_2Pt fragment inserts into the $(CF_3P)_5$ ring to give a $PtP(CF_3)[P(CF_3)]_2P(CF_3)$ metallacycle, which in turn decomposes by loss of $(CF_3P)_3$ to give the diphosphene products (eq 12). Although

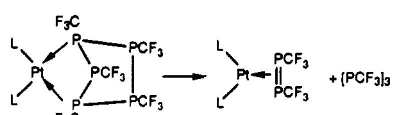
(12)

$(CF_3P)_3$ was not observed in the spectra of our reactions of the zerovalent metal substrates with CF_3 polyphosphines, it has been identified spectroscopically by Grobe et al.[36] as a major product (50%) of $SnCl_2$ reduction of CF_3PI_2 in THF at +25 °C. At this temperature the trimer was stable for approximately 24 h before it rearranges completely to a mixture of tetramer and pentamer.[36]

The stability of $(CF_3P)_3$ in benzene is unknown at this time. The rapid appearance of **9** from $[Pd(PPh_3)_4]$ and $(CF_3P)_{4,5}$ at +25 °C, in light of the slow isomerization/equilibrium of neat $(CF_3P)_{4,5}$ and the alternative mechanistic proposals represented in eqs 10–12, suggests two possibilities: either ring scission occurs as in eq 11 to give **9** or $[Pd(PPh_3)_4]$ somehow efficiently catalyzes the isomerization of $(CF_3P)_4$ into $(CF_3P)_5$ to give **9** via eqs 10 and 12. We favor the former mechanism, since we see no need to postulate a diminished stability for the complex $[Pd\{(CF_3P)_5\}(PPh_3)_2]$ relative to its analogues, **20** and **22–23**. Scheme II represents a

Scheme II

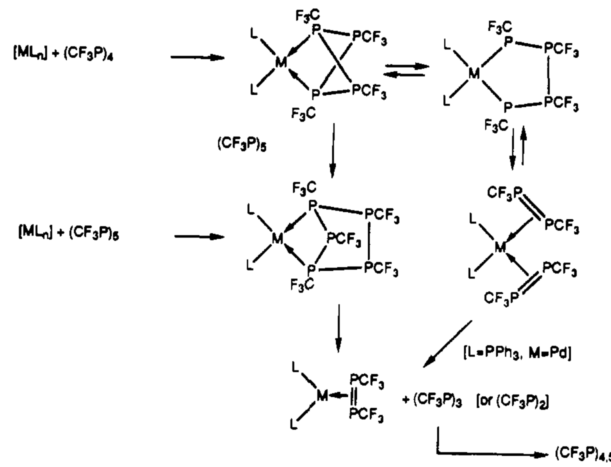

mechanistic summary of the reactions of the zerovalent nickel triad metal substrates with $(CF_3P)_{4,5}$.

This analysis suggests an alternative mechanism for the near-quantitative yield of **6** (relative to $K_2(Bu^tP)_2$) in the reaction of $[NiCl_2(PMe_3)_2]$ with $K_2(Bu^tP)_2$ in THF at −78 °C.[4] A disproportionation of the expected product **26** (eq 13) to give a

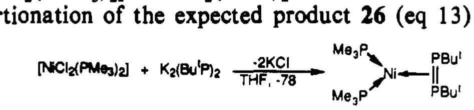
(13)

26

tris(diphosphene) analogue (**27**) of $[Ni(\eta^2\text{-}C_2H_4)_3]$ (eq 14) fol-

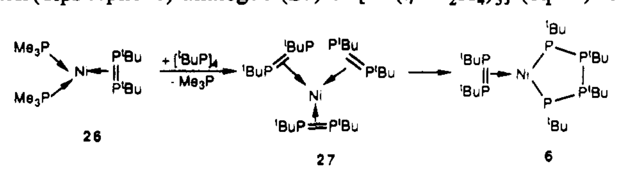
(14)

lowed by metallacycle formation (to give **6**) cannot be dismissed. However, a possibly more attractive mechanism is one which involves a slow partial decomposition of **26** to give $[^tBuP]_4$ (eq 15), which in turn reacts rapidly with the remaining **26** to give **6** by loss of both PMe_3 ligands (eq 16).

$$\mathbf{26} \longrightarrow [^tBuP]_4 + [Ni(PMe_3)_2]_n \quad (15)$$

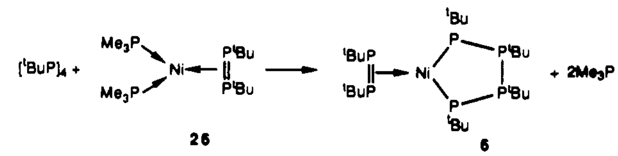
(16)

Intermetallic Transfer of the Diphosphene. The process indicated by eq 7 suggests that relative stabilities are sufficiently different and the system lability adequate to transfer the $CF_3P{=}PCF_3$ unit to different metals. It is clear that the diphosphene is more tightly bound to Pt(0) than Pd(0) and secondary complexation does not occur.

A formidable steric barrier may also operate here as a disincentive to cluster nucleation though no such trends were noted in the reactions of **3** and $[W(CO)_5(CH_3CN)]$ which eventually gave **10**.[2] On balance we think that the π-acidity, rather than the σ-donating ability of Pt(0)-bound $CF_3P{=}PCF_3$ is responsible for the observed pattern of reactivity and the increased stability of complexation with the more electron-rich (Pt) metal center. Thus, $CF_3P{=}PCF_3$ in **14**, by virtue of improved back-donation from Pt(0), is an impoverished π-acid. This and the characteristic poor nucleophilicity of perfluoromethyl-substituted phosphorus-(III)[40] are responsible for the absence of cluster nucleation.

(37) Burg, A. B.; Mahler, W. *J. Am. Chem. Soc.* **1961**, *83*, 2388.
(38) Wells, G. J.; Lee, H. P. K.; Peterson, L. K. *Chem. Commun.* **1967**, 894.
(39) Phillips, I. G.; Ball, R. G.; Cavell, R. G. *Inorg. Chem.* **1987**, *26*, 4074.
(40) Apel, J.; Grobe, J. *Z. Anorg. Allg. Chem.* **1979**, *453*, 53.

Further studies of the transfer reaction and additional complexation chemistry would appear to be worthwhile.

Acknowledgment. We thank the Natural Sciences and Engineering Research Council of Canada for financial support.

Registry No. **9**, 139732-78-8; **12**, 139732-79-9; **13**, 139732-80-2; **14**, 139732-81-3; **15**, 139732-82-4; **16**, 139732-83-5; **17a**, 139732-89-1; **17b**, 139732-90-4; **20**, 139732-86-8; **22**, 139732-84-6; **23**, 139732-85-7; **24**, 139732-87-9; **25**, 139732-88-0; $(CF_3P)_4$, 393-02-2; $(CF_3P)_5$, 745-23-3; $Pt(\eta^2\text{-}C_2H_4)(PPh_3)_2$, 12120-15-9; $Pt(PEt_3)_3$, 39045-37-9; $Pt(PEt_3)_4$, 33937-26-7; $Pt(PMe_2Ph)_4$, 33361-89-6; $Pt(PPh_3)_4$, 14221-02-4; $Pd(PPh_3)_4$, 14221-01-3; $Ni(dppe)_2$, 15628-25-8; $Pd(dppe)_2$, 31277-98-2.

Supplementary Material Available: Listings of crystallographic data, positional parameters, and anisotropic and equivalent isotropic thermal parameters (Tables S1–S3), root-mean-square amplitudes of thermal vibrations (Table S4), all interatomic distances (Table S5) and angles (Table S6), torsional angles (Table S7), and weighted least-squares planes (Table S8) (13 pages); a table of calculated and observed structure factors (Table S9) (41 pages). Ordering information is given on any current masthead page.

Contribution from the Dipartimento di Scienze Chimiche, Università di Catania, Viale A. Doria 8, 95125 Catania, Italy

Synthesis, Structure, and Bonding Properties of a New Volatile [*N*-*tert*-Butyl(1*H*-pyrrol-2-ylmethylene)aminato]thallium(I) Complex

Enrico Ciliberto,* Santo Di Bella, Antonino Gulino, and Ignazio L. Fragalà

Received May 15, 1991

The synthesis, characterization, structure, and bonding properties of the title complex are reported. The complex consists of monomeric units in the vapor phase. Geometrical structural parameters have been fully optimized using relativistic pseudopotential extended basis set gradient ab initio calculations. The most stable conformation was found to have a planar geometry with slightly different Tl–N bond distances. The metal–ligand bonding is σ-only in nature and involves strong mixing between several ligand-based valence molecular orbitals and both filled 5s and virtual 5p thallium atomic orbitals. The photoelectron spectra of the complex are in consistent agreement with this bonding description and further underscore the covalent nature of the metal–ligand bonding.

Introduction

The synthesis and structural characterizations of low-coordinated thallium(I) complexes has recently attracted considerable attention.[1] In addition, thallium(I) complexes act as mild transfer reagents for organic and inorganic ligands, yielding products unobtainable by conventional methods,[2] while volatile thallium compounds are better suited precursors for the MOCVD growth of thin films of superconducting Tl–Ba–Ca–Cu–O phases.[3] The metal–ligand bonding in thallium(I) complexes remains, however, still open to question, since only a few studies have been reported[4,5] and, in addition, relativistic effects due to the heavy metal certainly play a significant role.[4]

In this paper we report the synthesis, characterization, and electronic structure of a new thallium(I) volatile complex: [*N*-*tert*-butyl(1*H*-pyrrol-2-ylmethylene)aminato]thallium(I) (hereafter Tl(L), I).

The study combines experimental measurements using variable (He I and He II) photon source vapor-phase photoelectron (PE) spectroscopy and relativistic pseudopotential ab initio calculations to perform the geometry optimization, to study the ground-state electronic properties, and, together with ΔSCF calculations, to evaluate ionization energies (IEs).

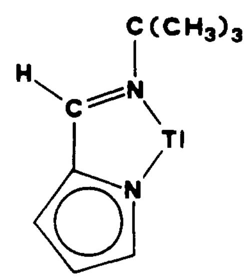

I

Experimental Section

Synthesis of Tl(L). The synthetic procedures were always conducted in strictly anhydrous solvents and under a prepurified N_2 atmosphere using the Schlenk method. Pyrrole-2-carboxaldehyde (9.5 g) (Aldrich Chemical Co.) and *tert*-butylamine (10.5 mL) (Fluka) were condensed into absolute ethanol (50 mL). The solution was allowed to stand for several hours at room temperature. Thallous ethoxide (1:1 molar ratio) (Fluka) was added dropwise. The white precipitate was filtered off and purified (yield 21%) by sublimation at 160 °C in vacuo (10^{-3} Torr); mp 260 °C dec. The compound appears almost insoluble in most common solvents. It slightly dissolves in DMSO even though any attempt to grow crystals by slow diffusion methodologies was unsuccessful. EI MS (18 eV), *m*/*z* (relative intensity): 354, 352 (M^+, 79, 39), 339, 337 ($(M - Me)^+$, 26, 11), 205, 203 (^{205}Tl, ^{203}Tl, 100, 62), 150 (HL^+, 18), 135 ($(HL - Me)^+$, 25). IR (Nujol mull): ν(C=N) 1608 cm^{-1}. ^1H NMR (DMSO-d_6, 250 MHz, TMS external reference): δ 1.28 (s, 9 H, CMe_3), 6.04 (q, 1 H, pyr), 6.54 (q, 1 H, pyr), 6.83 (d, 1 H, pyr), 8.65 (s, 1 H, CH). Anal. Found (calcd): Tl, 58.1 (57.8); C, 30.2 (30.6); N, 8.5 (7.9); H, 3.6 (3.7).

Physical Measurements. ^1H NMR spectra were obtained on a Bruker AC-250 spectrometer. IR spectra were recorded on a Perkin-Elmer 684 infrared spectrophotometer. The melting point was determined on a Mettler TA4000 microcalorimeter. Elemental microanalyses were performed in the Analytical Laboratories of the University of Catania. EI and FAB mass spectra (MS) were recorded on a Kratos MS 50 dou-

(1) Roesky, H. W.; Scholz, M.; Noltemeyer, M.; Edelmann, F. T. *Inorg. Chem.* **1989**, *28*, 3829.
(2) (a) Keefer, L. K.; Wang, S.; Anjo, T.; Fanning, J. C.; Day, C. S. *J. Am. Chem. Soc.* **1988**, *110*, 2800. (b) Gassman, P. G.; Winter, C. H. *J. Am. Chem. Soc.* **1986**, *108*, 4228.
(3) (a) Berry, A. D.; Holm, R. T.; Mowery, R. L.; Turner, N. H.; Fatemi, M. *Chem. Mater.* **1991**, *3*, 72. (b) Malandrino, G.; Richeson, D. S.; Marks, T. J.; DeGroot, D. C.; Schindler, J. L.; Kannewurf, C. R. *Appl. Phys. Lett.* **1991**, *58*, 182. (c) Hamaguchi, N.; Gardiner, R.; Kirlin, P. S.; Dye, R.; Hubbard, K. M.; Muenchausen, R. E. *Appl. Phys. Lett.* **1990**, *57*, 2136.
(4) (a) Schwerdtfeger, P.; Bowmaker, G. A.; Boyd, P. D. W.; Ware, D. C.; Brothers, P. J.; Nielson, A. J. *Organometallics* **1990**, *9*, 504. (b) Schwerdtfeger, P.; Boyd, P. D. W.; Bowmaker, G. A.; Mack, H. G.; Oberhammer, H. *J. Am. Chem. Soc.* **1989**, *111*, 15. (c) Balasubramanian, K. *Chem. Rev.* **1989**, *89*, 1801. (d) Canadell, E.; Eisenstein, O.; Rubio, J. *Organometallics* **1984**, *3*, 759.
(5) Janiak, C.; Hoffmann, R. *J. Am. Chem. Soc.* **1990**, *112*, 5924.

0020-1669/92/1331-1641$03.00/0